analytical chemistry

pubs.acs.org/ac Article

NMR for Mixture Analysis: Concentration-Ordered Spectroscopy

Bin Yuan, Zhiming Zhou, Bin Jiang, Ghulam Mustafa Kamal, Xu Zhang, Conggang Li, Xin Zhou, and Maili Liu*

Cite This: *Anal. Chem.* 2021, 93, 9697−9703 Read Online

ACCESS | Metrics & More | Article Recommendations | Supporting Information

ABSTRACT: A novel approach, concentration-ordered NMR spectroscopy (CORDY), is being proposed based on the principle that the ratio of the NMR peak area to its associated number of spins is proportional to the concentration of the assigned compound. Besides, prior information of chemical shift distribution and line shape characteristics of different chemical groups is utilized to shrink the solution space. CORDY generates a pseudo-two-dimensional NMR spectrum with chemical shifts in one axis and concentrations in the other, resulting in both separation and quantitation of components in complex samples. The method was validated by application to three samples—a model mixture containing six amino acids, sugar-free Red Bull, and human urine. It was demonstrated that CORDY could successfully separate the components with up to 2 orders of magnitude in the concentration dimension for the samples used in the current study. In addition, a combination of CORDY and DOSY (CORDY-DOSY) has been found to be more efficient in resolving the molecules with similar concentrations or self-diffusion coefficients.

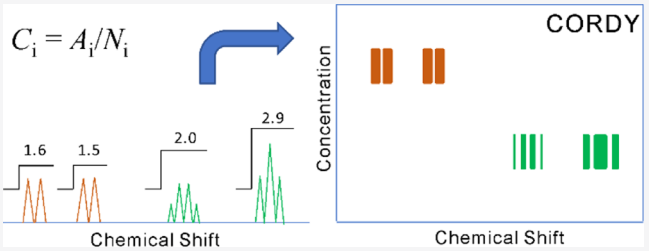

Nuclear magnetic resonance (NMR) spectroscopy[1−3] is considered to be a powerful tool in qualitative and quantitative analysis of mixtures and studies of molecular structures, interactions, and dynamics at atomic resolution. All this information is contained in NMR peaks and can be derived using appropriate pulse sequences that manipulate nuclear spins. In a simple case, the peak area in a fully relaxed single-pulse one-dimensional (1D) NMR spectrum is proportional to the number of spins and concentration of the molecule. It is a unique feature of NMR that the resonance intensity or peak area is molecule-independent, which ensures that concentrations of all components of a mixture can be determined quantitatively in one experiment.[4−6]

Identification of components in complex samples can be achieved by two- or higher dimensional (*n*D) correlation experiments.[7−9] The classical approaches for establishing the correlation are based on either spin−spin coupling[10] or dipole−dipole coupling,[11] resulting in correlation between the directly coupled functional groups or chains within a molecule, which has played a fundamental role in methodology and application of modern NMR spectroscopy. To ensure full assignment of NMR peaks of larger or complex molecules, two or more *n*D experiments are generally needed.

Diffusion-ordered NMR spectroscopy (DOSY)[12−16] is another type of method widely used for mixture analysis. DOSY separates chemical shift in one dimension and molecular self-diffusion coefficient in another. As the self-diffusion coefficient is a molecular property, all peaks from one molecule will be aligned accordingly in the DOSY plot and therefore can be distinguished from the other components. In addition, combination of diffusion- and relaxation-weighted NMR has been proved to be a valuable technique for improving the separation of biological mixtures.[17−19] The third type of the methods, namely, statistical total correlation spectroscopy (STOCSY),[20−23] was developed by Nicholson's group for identifying potential biomarkers and the molecules involved in the same pathway. STOCSY[20] is based on the principle that in a set of NMR spectra, intensities of the peaks from one molecule or from the molecules that are involved in the same pathway are linearly correlated. The covariation can be measured statistically and is used to generate pseudo-2D plot of STOCSY.[20] In addition, electrophoretic mobility has also been utilized in NMR (mobility spectroscopy, MOSY) to separate the charged molecules in solution.[24−27] However, due to the limited dynamic ranges, the molecules with similar self-diffusion coefficient constants and electronic changes could not be fully resolved by DOSY, MOSY, and STOCSY. Herein, we proposed a novel approach for constructing concentration-ordered NMR spectroscopy (CORDY) for simultaneously separating and quantitating the signals of the components of a mixture.

Received: February 23, 2021
Accepted: June 25, 2021
Published: July 6, 2021

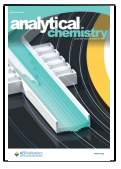

https://doi.org/10.1021/acs.analchem.1c00831
Anal. Chem. 2021, 93, 9697−9703

EXPERIMENTAL SECTION

Sample Preparation. Amino acids, L-histidine, L-threonine, L-arginine, L-glycine, L-tryptophan, and L-glutamic, and D_2O (99.9%) were purchased from Sigma (St. Louis, MO) and Biosharp (Hefei, China). Double-distilled water was prepared on a Millipore system and used as a solvent for amino acids. Energy drink sugar-free Red Bull was manufactured in Switzerland according to the information printed on the label on the can and purchased from Jingdong Worldwide (Jingdong import cross-border e-commerce platform). Human urine was taken from a healthy male volunteer and filtered using a 0.22 μM microfiltration membrane.

The urine sample consisted of 250 μL of D_2O, 300 μL of human urine, and sodium azide of 0.05% w/v. The energy drink sample consisted of 100 μL of D_2O and 400 μL of Red Bull. The amino acid mixture was prepared in aqueous solution with addition of 17.8% (v/v) D_2O for field lock. The concentration of threonine was 4.85 mM and used as an internal reference.

NMR Spectroscopy. NMR experiments were performed on Bruker Avance spectrometers (Bruker Biospin, Germany) operating at an ^1H frequency of 599.81 MHz (for amino acids), 949.9 MHz (for human urine)m and 600.13 MHz (for Red Bull) at 25 °C, all equipped with a cryoprobe. The NMR experiments on the 950 MHz spectrometer were performed at the NMR facility of the National Center for Protein Sciences at Peking University, and the other experiments were performed at National Center for Magnetic Resonance in Wuhan.

The fully relaxed 1D NMR spectra were acquired into 64k complex data points for derivation of CORDY. The water signal was suppressed with pre-saturation (for urine) and a modified "Pre-SAT180"[28] sequence (Figure S1, for amino acids and Red Bull). The spectral window and relaxation delay and saturation times were, respectively, 21,020 Hz, 14 s, and 2.3 s for amino acids, 9591 Hz, 12 s, and 4.5 s for Red Bull, and 15,244 Hz, 13 s, and 2 s for urine. To minimize the potential artifacts associated with data acquisition, four dummy scans were performed. Before Fourier transformation, an exponential line broadening of 0.3 Hz was applied to the time domain data and zero-filled to 128k (for amino acids and Red Bull) or 256k (for urine). The chemical shift of the threonine CH_3 group at δ 1.316 was chosen as an internal reference. The peak area was integrated manually after careful phase and baseline correction. The overlapped peaks were deconvoluted using the module "line shapes" of Bruker Topspin 4.0. For the complex spectrum of urine, we used commercial software, MestReNova, which automatically deconvolutes the overlapped peaks.[29,30]

Diffusion Experiments. The BPP-LED pulse sequence[31] was used to measure the self-diffusion coefficients and to construct DOSY conventionally. The spectral windows, time domain data points, and Fourier transformation were the same as 1D NMR. The other parameters were a diffusion time of 80 ms, Eddy current delay of 5 ms, gradient pulse duration of 2 ms, and relaxation delay of 2 s. Eight gradient strengths linearly spaced between 1.49 and 47.03 Gauss/cm (for Red Bull) and 1.51 and 47.84 Gauss/cm (for amino acids) were used with 32 (for Red Bull) and eight (for amino acids) scans for each gradient. The diffusion coefficients (D) are derived for the corresponding peaks using the module "T1T2" of Bruker Topspin 4.0.

BASICS OF CONCENTRATION-ORDERED SPECTROSCOPY (CORDY)

For a molecule consisting of m non-equivalent functional groups (CH, CH_2, or CH_3), there would be m peaks in its ^1H NMR spectrum. Therefore, a mixture with l components will have $m{\cdot}l$ peaks at the maximum. The peak area, A_i, is proportional to the number of chemically equivalent protons (N_i) and molar concentration (C_i), that is, $A_i = kN_iC_i$. According to the NMR principle, the resonance index (k) is non-discriminative for all peaks and molecules and thus could be treated as unit (1.0). In this case, C_i represents relative concentration

$$C_i = A_i/N_i \tag{1a}$$

$$N_i = \mathrm{round}(A_i/C_i, 0) \tag{1b}$$

where $\mathrm{round}(A_i/C_i, 0)$ is an operation of rounding off A_i/C_i to the nearest integer. For ^1H NMR, the common value of N_i is 1, 2, or 3 corresponding to CH, CH_2, or CH_3. The number can be doubled (2, 4, and 6) or tripled (3, 6, and 9) in the case of magnetic equivalence. Once the proton number (N_i) is obtained, it is possible to get the concentration (C_i) associated with each peak (eqs 1a and 1b). By plotting the chemical shift against the derived C_i, one gets a pseudo-2D spectrum of CORDY.

For constructing CORDY, the key point is the determination of N for each peak. The general knowledge of NMR[9,32] implies that peaks of CH_3 normally appear in a chemical shift range of δ 0.0–δ 4.0 with the line shape of singlet, doublet, or triplet. Peaks of CH and CH_2 can be found in the range of δ 1.0–δ 15.0 and δ 0.6–δ 5.5, respectively, with variable line shapes from singlet to multiplet. These essential properties are used as the first criteria. For a mixture with $m{\cdot}l$ peaks, it is recommended to find a peak (A_j) with a known proton number (N_j) and to use the ratio as a divisor

$$C_i/C_j = (N_i/A_i)/(N_j/A_j) \tag{2}$$

If peaks i and j belong to a same molecule ($C_i = C_j$), one gets eqs 3a and 3b

$$N_jA_i/A_j = N_i \pm \Delta_{i,j} \tag{3a}$$

$$N_i = \mathrm{round}(N_jA_i/A_j, 0) \tag{3b}$$

where Δ is the allowed error and is used as a threshold ($\leq$0.1 or $\leq$5%) for defining the proton number. With the obtainable peak areas and the finite number of protons associated with each peak, one can get the N for each peak using eqs 3a and 3b, the second criteria. Therefore, the peaks with N = 1, 2, and 3 and $\Delta \leq 0.1$ (5%) are likely to come from a same molecule or component. A short program was written accordingly to define the proton number and to group and assign the peaks (Scheme 1).

Constructing CORDY. The first step for constructing CORDY is to prepare a working table containing the NMR peak identification (id), chemical shift, area (A_i), line shape, and potential spin (^1H) number (N_i). The self-diffusion coefficient may also be included as an additional supplement. All this information can be obtained from quantitative and diffusion NMR experiments and general knowledge of NMR and used as input for the processing.

The next step, also the main part of the processing, is to define values of the N_{ij} for each peak i of component j,

https://doi.org/10.1021/acs.analchem.1c00831
Anal. Chem. 2021, 93, 9697–9703

Scheme 1. Flowchart for Constructing CORDY

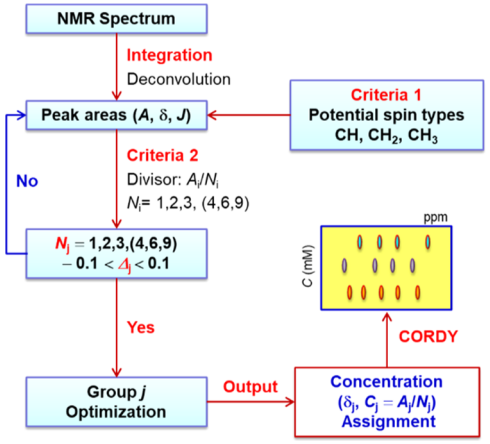

respectively. It is recommended to start with a peak of the aromatic (N_i = 1) or methyl (N_i = 3) region and to use the corresponding C_i (= A_i/N_i) as a divisor applied to all peaks (eq 4a). Depending upon the properties, the peaks with N = 1, 2, or 3, $|\Delta| \leq 0.1$ (or 5%) could be considered as originating from the same group or component j. The deviation (Δ_{ij}, eq 4b) and mean concentration (C_j, eq 4c) can be derived as

$$N_{ij} = \text{round}(A_{ij}/C_i, 0) \tag{4a}$$

$$\Delta_{ij} = A_{ij}/C_j - N_{ij} \tag{4b}$$

$$C_j = \frac{1}{m}\sum_{i=1}^{m}(A_{ij}/N_{ij}) \tag{4c}$$

where the deviation Δ_{ij} represents the linewidth along concentration axis. This process is repeated until all the peaks are grouped or assigned to different components.

Mathematically, the searching processes correspond to finding the greatest common divisors C_j for each component and minimizing the cost function $f_{\min}$

$$f_{\min} = \sum_{j=1}^{l}\left[\sum_{i=1}^{m}|A_{ij}/C_j - N_{ij}|\right] = \sum_{ij}|\Delta_{ij}| \tag{5}$$

When tuning the peak between the groups to minimize $f_{\min}$, one should pay attention to the requirements, such as N = 1, 2, or 3, $|\Delta| \leq 0.1$ (or 5%) and peak properties. To speed up the searching process, one could exclude the grouped peaks from the working list and search within the remains. Once the peaks are grouped or assigned to different components, one can construct the CORDY, $S(\delta, C)$, by plotting the chemical shift against the derived concentration

$$S(\delta, C) = \sum_{ij}\frac{S_{ij}(\delta)}{A_{ij}}N_{ij}\exp\left(\frac{-(C - C_{ij})^2}{2(C_j\Delta)^2}\right) \tag{6}$$

$$C_{ij} = C_j\left(1 + \frac{A_{ij}}{C_j} - N_{ij}\right) \tag{7}$$

where $S(\delta)$ represents the 1D NMR spectrum. The vertical scale of CORDY corresponds to concentration by default. It can be the absolute concentration if an internal or external ref 33 is used, similar to conventional quantitative NMR. For simplicity, "$C_j\Delta$" is chosen as the error instead of standard deviation of peaks' concentration.

The algorithms are written in MATLAB and still being improved. The code is free for academic use upon request by email. The whole procedure is now semi-automatic and can be developed to be completely automatic in the future using scripts in commercial software (e.g., MestReNova NMR).

RESULTS AND DISCUSSION

Figure 1 shows the CORDY of the amino acids. The procedure starts with the acquisition of a fully relaxed ^{1}H NMR spectrum

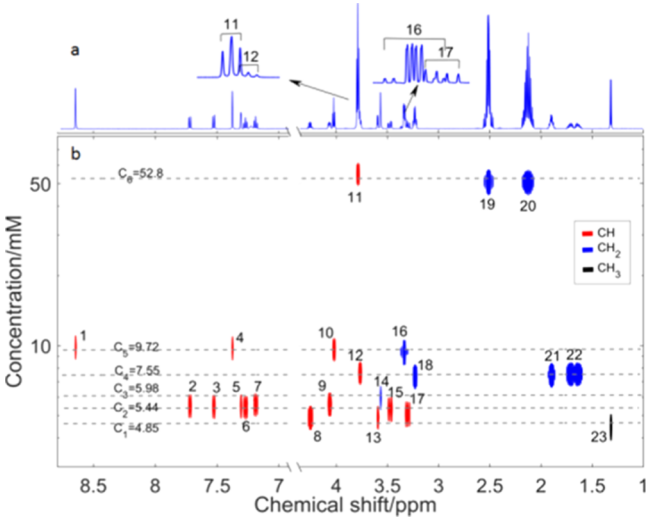

Figure 1. (a) High-resolution ^{1}H NMR spectrum showing the spectral region (1.0−8.7 ppm) with two enlarged parts after resolution enhancement and its CORDY plot (b). The peaks are assigned as follows: L-threonine (**8**, **13**, and **23**), L-glutamate (**11**, **19**, and **20**), L-histidine (**1**, **4**, **10**, and **16**), L-tryptophan (**2**, **3**, **5**, **6**, **7**, **9**, **15**, and **17**), L-arginine (**12**, **18**, **21**, and **22**), and glycine (**14**). The concentration value of components is referenced to that of L-threonine (4.85 mM). The linewidth was defined by Δ; in this case, the maximum error of 5% was used for all peaks along the concentration dimension.

(Figure 1a). After careful correction of the phase and baseline, the integral values of 23 peaks were obtained manually (Table S1). Among these peaks, two overlapped regions, peaks **11** & **12** and **16** & **17**, were resolved by deconvolution.[34,35] The peak **1** at δ 8.642 with singlet(s) line shape is possibly a CH (N_1 = 1) and an ideal candidate to start the search. When A_1 (0.696) was used as a divisor (eqs 3a, 3b, 4a, 4b, and 4c), three peaks, **4** (δ 7.376, s, A_4 = 0.690), **10** (δ 4.022, t-triplet, A_{10} = 0.679), and **16** (δ 3.334, m-multiplet, A_{16} = 1.345), had $N_{4,10,16}$ = 1, 1, and 2 and $\Delta \leq 0.1$, respectively, and could be classified in one group according to the 1st and 2nd criteria. The other peaks had either an impractical proton number or $\Delta > 0.1$. This component corresponds to histidine. Once the group is defined, the average value of the peak area to the spin number is calculated, and the value is directly correlated to the concentration (eqs 1a and 1b) of the component. In the next step when peak **2** (δ 7.718, d, N_2 = 1, A_2 = 0.388) was used as a divisor, the values of N for seven peaks at δ 7.525 (**3**, d, A_3 = 0.386), δ 7.307 (**5**, s, A_5 = 0.387), δ 7.270 (**6**, t, A_6 = 0.383), δ 7.187 (**7**, t, A_7 = 0.393), δ 4.066 (**9**, dd, A_9 = 0.395) δ 3.475 (**15**, dd, A_{15} = 0.376), and δ 3.301 (**17**, dd, A_{17} = 0.358) were found to be 1:1:1:1:1:1:1 (CH). This component is assigned

https://doi.org/10.1021/acs.analchem.1c00831
Anal. Chem. 2021, 93, 9697−9703

to tryptophan. Next, we took peak **22** at δ 1.673 (m) as an example for starting the search with a methylene group. This assumption is reasonable because of its symmetrical line shape in the profile but different *J*s from two halves can be inferred to arise from two chemically non-equivalent protons strongly coupled with each other but weakly coupled with other protons. When this peak (N_{22} = 2, A_{22} = 1.063) was applied, we found that the values of *N* for three peaks at δ 3.767 (**12**, t, A_{12} = 0.538), δ 3.232 (**18**, t, A_{18} = 1.05), and δ 1.898 (**21**, m, A_{21} = 1.06) were found to be 1, 2, and 2, respectively. These peaks were assigned to arginine. Similarly, three subgroups, group 1 (**11**, A_{11} = 3.865, **19**, A_{19} = 7.295, and **20**, A_{20} = 7.286), group 2 (**14**, A_{14} = 0.842), and group 3 (**8**, A_8 = 0.346, **13**, A_{13} = 0.346, and **23**, A_{23} = 0.998), were found, which corresponded to L-threonine, glycine, and L-glutamate, respectively. It should be indicated that the divisor may be varied within a defined error to see whether or not more peaks belong to one component. This is exactly what our customized local optimization algorithm does. However, if one peak satisfies both criteria belonging to two or more components, our customized algorithm for global optimization will select and recommend the solution with minimal error (eq 5). After *N* was defined for each peak, relative concentrations were derived directly for all components using eq 1a (Table S1), which in turn were used to construct CORDY. The absolute concentration of other amino acids can be determined by referring to that of L-threonine (4.85 mM). It can be seen from Figure 1 that CORDY provides a separation capacity of at least 1 order of magnitude in the *C* dimension, resulting in a significant partition of six components of the sample.

To further demonstrate the usefulness of CORDY, an energy drink, namely, sugar-free Red Bull, was taken as another example. After careful phase and baseline correction of a fully relaxed ^{1}H NMR spectrum (Figure 2a), 22 peaks were integrated manually (Table S2) where the overlapped peaks **11** and **12** were resolved by deconvolution as mentioned before. The peak **1** at δ 8.943 with singlet(s) line shape is possibly a CH (N_1 = 1) and an ideal candidate to start the search. When A_1 (2.46) was used as a divisor (eqs 3a and 3b), three peaks—**2** (δ 8.703, d), **3** (δ 8.405, d), and **5** (δ 8.716, t)—had $N_{2,3,5}$ = 1 and $\Delta \leq 0.1$, respectively, and could be classified in one group according to the 1st and 2nd criteria. The other peaks had either an impractical proton number or $\Delta > 0.1$. Referring to ingredients of Red Bull, chemical shifts, line shapes of these peaks, and the literature,[36] the peaks **1**, **2**, **3**, and **5** were assigned to 2-H, 6-H, 4-H, and 5-H of niacin (vitamin B3), respectively. Once the group is defined, the average value of the peak area divided by the spin number can be calculated and is directly correlated to concentration (eqs 1a and 1b) of the component. The mean value of niacin was set to 1.0 for internal reference. Using peak **4** (δ 7.804, s, N_4 = 1, A_4 = 15.0) as a divisor, the value of *N* for three peaks at δ 3.861 (**7**, s), δ 3.441 (**12**, s), and δ 3.259 (**14**, s) was found to be 3 (CH_3). These four peaks were originated from caffeine[37,38] (8-CH, 7-CH_3, 1-CH_3, and 3-CH_3, respectively), an indispensable component of Red Bull with a relative concentration of 6.02. We took peak **22** at δ 1.044 (d) as an example for starting the search with a methyl group. When this peak (N_{22} = 3, A_{22} = 530.4) was applied, it was found that the peaks **8** (δ 3.786, m, N_8 = 1), **11** (δ 3.448, dd, N_{11} = 1), and **13** (δ 3.348, dd, N_{13} = 1) belonged to the same group of **22** with a relative concentration of 73.7. The peak **8** was assigned to 2-CH, **11** and **13** were assigned to two geminate protons 1-CH_2, and **22** was assigned to 3-CH_3 of propylene glycol.[39,40] Using the same procedure, we were able to separate the leftover assigned peaks into four groups, defined the *N* and relative concentration, and assigned them[36,41,42] to acesulfame-K (N_6 = 1, N_{18} = 3), arginine (N_9 = 1, N_{15} = 2, N_{19} = 2, N_{20} = 2), citrate (N_{16} = 2, N_{17} = 2), and ethanol (N_{10} = 1, N_{21} = 3). The typical chemical shifts (δ 2.810 and δ 2.687) and coupling constant (*J* = 15.5 Hz) make it easy to assign the peaks to two geminate protons 1,3-CH_2 of citrate.[36] After *N* was defined for each peak, relative concentrations, referring to niacin as 1.00, were derived directly for all components using eq 1a (Table S2), which in turn were used to construct CORDY. It can be seen from Figure 2 that CORDY provides a separation capacity of at least 2 orders of magnitude in the *C* dimension, resulting in a good separation of seven components of the sample.

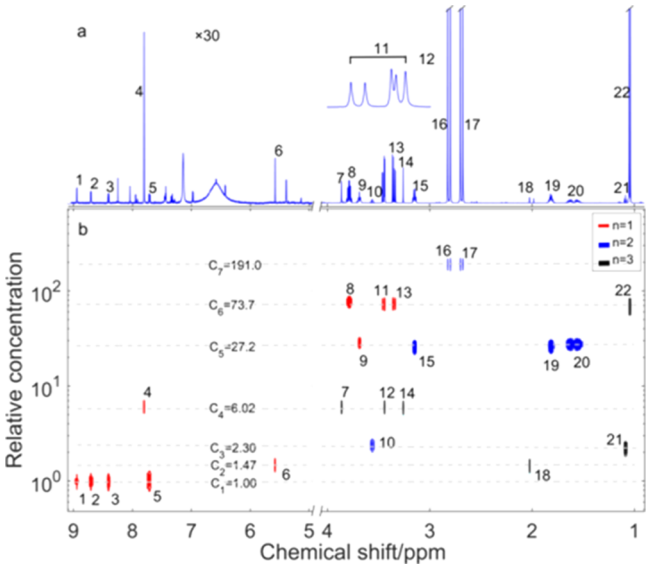

Figure 2. High-resolution fully relaxed ^{1}H NMR spectrum (a) of sugar-free Red Bull and its CORDY (b). The vertical scale of 1D NMR was magnified by 30 times on the left side. The overlapped peaks **11** and **12** are enlarged and plotted as insets. The peaks are separated into seven groups according to relative concentrations and assigned to niacin (1, 2, 3, and 5; C = 1.0 as a reference), caffeine (4, 7, 12, and 14), acesulfame-K (6 and 18), arginine (9, 15, 19, and 20), ethanol (10 and 21), citrate (16 and 17), and propylene glycol (8, 11, 13, and 22). The linewidth along the concentration dimension was defined by Δ.

For comparison, DOSY was conducted and is shown in Figure S2, which separated the seven components into four groups, with ethanol alone in a group, niacin, acesulfame-K, and propylene glycol in the second group, caffeine in the third group, and citrate and arginine in the fourth group, possibly due to the small dynamic range of the *D* values ($6.3-10 \times 10^{-10}$ m^2/s). In general, components with similar self-diffusion coefficients or concentrations could not be resolved by DOSY.

For a more complex mixture, human urine was taken as an example, and the low-field region (δ 6.3–δ 9.4) was selected for analysis. The analysis is greatly simplified because only CH groups exist. We employed commercial software MestReNova (V.14.0.0) to deconvolute the spectrum[29] automatically and picked out 47 peaks regardless of overlaps (Table S3). The plot of CORDY is shown in Figure 3, together with the 1D spectrum, where the equivalent CH (*N* = 2) was defined based on the ratio of the peak area and referring to the general knowledge. For example, in hippurate, the typical chemical

https://doi.org/10.1021/acs.analchem.1c00831
Anal. Chem. 2021, 93, 9697−9703

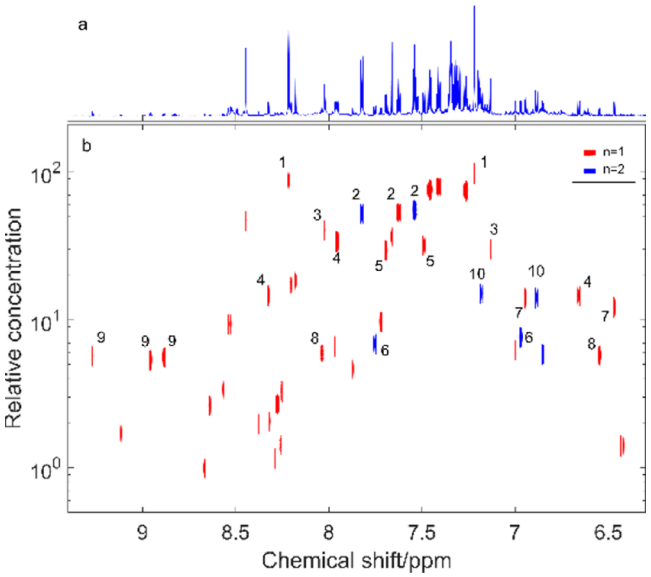

Figure 3. ^{1}H CORDY plot (b) of the human urine spectrum (a) of the CH region (δ 6.3−9.4). Peaks from 10 molecules (label 1−10) were identified. The linewidth along the concentration dimension was defined by Δ.

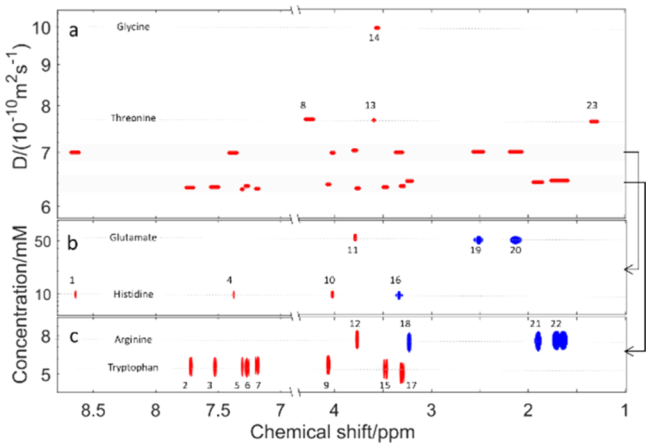

Figure 4. (a) Plot of self-diffusion coefficients against the chemical shift (DOSY) of human urine. The overlapped regions containing L-glutamate (**11**, **19**, and **20**), L-histidine (**1**, **4**, **10**, and **16**), L-tryptophan (**2**, **3**, **5**, **6**, **7**, **9**, **15**, and **17**), and L-arginine (**12**, **18**, **21**, and **22**) were marked by gray traces. Glycine (**14**) and L-threonine (**8**, **13**, and **23**) were separated from others. (b,c) CORDY plots of the marked regions, demonstrating the usefulness of the combination of CORDY and DOSY. The linewidth along the concentration dimension was defined by Δ.

shifts, coupling pattern, and peak area ratio make it easy to identify its three peaks at δ 7.823 (d, $A_{2,6}$ = 262.9, N = 2), δ 7.624 (t, $A_{2,6}$ = 134.0, N = 1), and δ 7.641 (t, $A_{2,6}$ = 2878.8, N = 2). Similarly, the peaks from 10 molecules were identified and labeled in the figure, and the assignment was confirmed by TOCSY.

The results stated above imply that CORDY could be useful for analyzing mixtures with a high dynamic content up to two orders of magnitudes. Two components with similar concentration may fail to be resolved but could be separated by another dimension, such as the diffusion coefficient. In practice, it is less likely to have two components with both a similar concentration and diffusion coefficient. Therefore, combination of CORDY and DOSY, 3D CORDY-DOSY, could enhance the separation abilities of the two approaches. CORDY-DOSY is obtainable by post-processing with a combination of CORDY and DOSY. This provides flexible options for processing and displaying the full range or part of the concentration and the self-diffusion coefficient, with high resolution in the chemical shift dimension.

To demonstrate the usefulness of 3D CORDY-DOSY, we applied the approach to the amino acid mixture. As shown in Figure 4a, DOSY fully resolved glycine (**14**) and threonine (**8**, **13**, and **23**). However, histidine (**1**, **4**, **10**, and **16**), glutamate (**11**, **19**, and **20**), tryptophan (**2**, **3**, **5**, **6**, 7, **9**, **15**, and **17**), and arginine (**12**, **18**, **21**, and **22**) were overlapped in the diffusion dimension, as marked with gray traces in the figure. The two overlapped regions were nicely separated by CORDY (Figure 4b,c). In addition, the concentrations of threonine (4.85 mM) and tryptophan (5.44 mM) were close and hardly distinguishable in CORDY (Figure 1) but were unambiguously separated in DOSY (Figure 4). Furthermore, niacin and propylene glycol and caffeine and arginine in Red Bull are indistinguishable in DOSY (Figure S2) as they have close self-diffusion coefficient values; these two pairs are clearly resolved in CORDY (Figure 2b).

CONCLUSIONS

A novel approach, CORDY, was proposed based on the principle that the ratio of the peak area to its associated spin number is proportional to the concentration of the molecule, a unique property of NMR spectroscopy. The new method was validated on a model mixture consisting of six amino acids, human urine, and a sugar-free energy drink, Red Bull. It was demonstrated that CORDY provides a new way for simultaneous quantitation of components and separation of NMR peaks of a mixture, resulting in a dynamic range of more than 2 orders of magnitude in the concentration dimension and high resolution in the chemical shift dimension. In addition, CORDY could be combined with other techniques (here, DOSY) to further resolve the components with similar concentrations or self-diffusion coefficients. However, we should indicate that similar to other *n*D NMR techniques, the proposed method, CORDY, is limited by heavily overlapped peaks. In such a case, advanced deconvolution algorithms[29,43] could resolve part of the problem. Another obstacle could be defining the spin number N, especially for the inexperienced NMR users. Fortunately, the majority of ^{1}H NMR peaks have a proton number of 1, 2, or 3, and the peak of CH appears at the low-field region, with CH_2 at middle and CH_3 at the high field. It should be kept in mind that there are cases where the proton number could be doubled or even more, such as a tertiary butyl group (N = 9) and a cyclopentadienyl ligand (N = 5) as reminded by the reviewer. These general properties should be beneficial. Furthermore, we showed that a combination of CORDY and DOSY, 3D CORDY-DOSY, can significantly enhance the resolution. Principally, we expected that CORDY can be combined with the other *n*D NMR methods, such as gradient-enhanced COSY that only takes a few minutes, and link the uncoupled spins within a molecule. Finally, we should point out that CORDY may perform better for quantitative ^{13}C NMR.[44]

https://doi.org/10.1021/acs.analchem.1c00831
Anal. Chem. 2021, 93, 9697−9703

■ ASSOCIATED CONTENT

Supporting Information

The Supporting Information is available free of charge at https://pubs.acs.org/doi/10.1021/acs.analchem.1c00831.

Modified pulse sequence of Pre-SAT180, DOSY of Red Bull, and NMR data used to construct CORDY of amino acids, Red Bull, and human urine (PDF)

NMR experiments, modified Pre-SAT180 pulse sequence, and plot of diffusion coefficients as a function of the chemical shift (DOSY) for the peaks of the Red Bull sample (PDF)

N values of peaks of L-glutamate, L-histidine, threonine, and tryptophan and related data (XLSX)

■ AUTHOR INFORMATION

Corresponding Author

Maili Liu − *State Key Laboratory of Magnetic Resonance and Atomic and Molecular Physics, National Center for Magnetic Resonance in Wuhan, Wuhan Institute of Physics and Mathematics, Innovation Academy for Precision Measurement Science and Technology, Chinese Academy of Sciences−Wuhan National Laboratory for Optoelectronics, Huazhong University of Science and Technology, Wuhan 430071, China; University of Chinese Academy of Sciences, Beijing 10049, China;* orcid.org/0000-0002-9359-915X; Email: ml.liu@apm.ac.cn

Authors

Bin Yuan − *State Key Laboratory of Magnetic Resonance and Atomic and Molecular Physics, National Center for Magnetic Resonance in Wuhan, Wuhan Institute of Physics and Mathematics, Innovation Academy for Precision Measurement Science and Technology, Chinese Academy of Sciences−Wuhan National Laboratory for Optoelectronics, Huazhong University of Science and Technology, Wuhan 430071, China; University of Chinese Academy of Sciences, Beijing 10049, China;* orcid.org/0000-0003-1270-4024

Zhiming Zhou − *State Key Laboratory of Magnetic Resonance and Atomic and Molecular Physics, National Center for Magnetic Resonance in Wuhan, Wuhan Institute of Physics and Mathematics, Innovation Academy for Precision Measurement Science and Technology, Chinese Academy of Sciences−Wuhan National Laboratory for Optoelectronics, Huazhong University of Science and Technology, Wuhan 430071, China; University of Chinese Academy of Sciences, Beijing 10049, China*

Bin Jiang − *State Key Laboratory of Magnetic Resonance and Atomic and Molecular Physics, National Center for Magnetic Resonance in Wuhan, Wuhan Institute of Physics and Mathematics, Innovation Academy for Precision Measurement Science and Technology, Chinese Academy of Sciences−Wuhan National Laboratory for Optoelectronics, Huazhong University of Science and Technology, Wuhan 430071, China; University of Chinese Academy of Sciences, Beijing 10049, China*

Ghulam Mustafa Kamal − *Department of Chemistry, Khwaja Fareed University of Engineering and Information Technology, Rahim Yar Khan 64200, Pakistan*

Xu Zhang − *State Key Laboratory of Magnetic Resonance and Atomic and Molecular Physics, National Center for Magnetic Resonance in Wuhan, Wuhan Institute of Physics and Mathematics, Innovation Academy for Precision Measurement Science and Technology, Chinese Academy of Sciences−Wuhan National Laboratory for Optoelectronics, Huazhong University of Science and Technology, Wuhan 430071, China; University of Chinese Academy of Sciences, Beijing 10049, China*

Conggang Li − *State Key Laboratory of Magnetic Resonance and Atomic and Molecular Physics, National Center for Magnetic Resonance in Wuhan, Wuhan Institute of Physics and Mathematics, Innovation Academy for Precision Measurement Science and Technology, Chinese Academy of Sciences−Wuhan National Laboratory for Optoelectronics, Huazhong University of Science and Technology, Wuhan 430071, China; University of Chinese Academy of Sciences, Beijing 10049, China;* orcid.org/0000-0002-5798-1722

Xin Zhou − *State Key Laboratory of Magnetic Resonance and Atomic and Molecular Physics, National Center for Magnetic Resonance in Wuhan, Wuhan Institute of Physics and Mathematics, Innovation Academy for Precision Measurement Science and Technology, Chinese Academy of Sciences−Wuhan National Laboratory for Optoelectronics, Huazhong University of Science and Technology, Wuhan 430071, China; University of Chinese Academy of Sciences, Beijing 10049, China;* orcid.org/0000-0002-5580-7907

Complete contact information is available at: https://pubs.acs.org/10.1021/acs.analchem.1c00831

Notes

The authors declare no competing financial interest.

■ ACKNOWLEDGMENTS

This research was funded by the National Key R&D Program of China (2018YFE02202300, 2018YFA0704002, and 2017YFA0505400), National Natural Science Foundation of China (21735007, 21991080, and 21921004), and CAS Key Research Program of Frontier Sciences (QYZDJ-SSW-SLH027). The authors thank Professor Changwen Jin and Dr. Xiaogang Niu from Beijing University, Professor Yunfei Hu from Innovation Academy for Precision Measurement Science and Technology for helping with the experimental setup at 950 MHz and valuable discussion. Special thanks to the reviewers for their valuable comments and providing the molecules with $N = 5$ and 9.

■ REFERENCES

(1) Abragam, A. *The Principles of Nuclear Magnetism*; Oxford University Press: London, 1961.

(2) Ersnt, R. R.; Bodenhausen, G.; Wokaun, A. *Principles of Nuclear Magnetic Resonance in One and Two Dimensions*; Clarendon Press, Oxford University Press: New York and London, 1987; p 610.

(3) Callaghan, P. T. *Principles of Nuclear Magnetic Resonance Microscopy*; Claredon Press: Oxford, 1993.

(4) Simmler, C.; Napolitano, J. G.; McAlpine, J. B.; Chen, S.-N.; Pauli, G. F. *Curr. Opin. Biotechnol.* **2014**, *25*, 51−59.

(5) Li, X.; Hu, K. *Annual Reports on NMR Spectroscopy*; Webb, G. A., Ed.; Elsevier Inc, 2017; Vol. *90*, pp 85−143.

(6) Mulder, F. A. A.; Tenori, L.; Luchinat, C. *Angew. Chem., Int. Ed.* **2019**, *58*, 15283−15286.

(7) Aue, W. P.; Bartholdi, E.; Ernst, R. R. *J. Chem. Phys.* **1976**, *64*, 2229−2246.

(8) Nicholson, J. K.; Wilson, I. D. *Prog. Nucl. Magn. Reson. Spectrosc.* **1989**, *21*, 449−501.

(9) Fan, T. *Prog. Nucl. Magn. Reson. Spectrosc.* **1996**, *28*, 161−219.

(10) Braunschweiler, L.; Ernst, R. R. *J. Magn. Reson.* **1983**, *53*, 521−528.

(11) Jeener, J.; Meier, B. H.; Bachmann, P.; Ernst, R. R. *J. Chem. Phys.* **1979**, *71*, 4546−4553.
(12) Stejskal, E. O.; Tanner, J. E. *J. Chem. Phys.* **1965**, *42*, 288−292.
(13) Morris, K. F.; Johnson, C. S. *J. Am. Chem. Soc.* **1992**, *114*, 3139−3141.
(14) Barjat, H.; Morris, G. A.; Swanson, A. G. *J. Magn. Reson.* **1998**, *131*, 131−138.
(15) Loening, N. M.; Keeler, J.; Morris, G. A. *J. Magn. Reson.* **2001**, *153*, 103−112.
(16) Johnson, C. S. *Prog. Nucl. Magn. Reson. Spectrosc.* **1999**, *34*, 203−256.
(17) Liu, M.; Nicholson, J. K.; Lindon, J. C. *Anal. Chem.* **1996**, *68*, 3370−3376.
(18) Zhang, X.; Li, C.-G.; Ye, C.-H.; Liu, M.-L. *Anal. Chem.* **2001**, *73*, 3528−3534.
(19) Nilsson, M.; Botana, A.; Morris, G. A. *Anal. Chem.* **2009**, *81*, 8119−8125.
(20) Cloarec, O.; Dumas, M.-E.; Craig, A.; Barton, R. H.; Trygg, J.; Hudson, J.; Blancher, C.; Gauguier, D.; Lindon, J. C.; Holmes, E.; Nicholson, J. *Anal. Chem.* **2005**, *77*, 1282−1289.
(21) Maher, A. D.; Fonville, J. M.; Coen, M.; Lindon, J. C.; Rae, C. D.; Nicholson, J. K. *Anal. Chem.* **2012**, *84*, 1083−1091.
(22) Robinette, S. L.; Lindon, J. C.; Nicholson, J. K. *Anal. Chem.* **2013**, *85*, 5297−5303.
(23) Holmes, E.; Cloarec, O.; Nicholson, J. K. *J. Proteome Res.* **2006**, *5*, 1313−1320.
(24) He, Q.; Johnson, C. S. *J. Magn. Reson.* **1989**, *81*, 435−439.
(25) Morris, K. F.; Johnson, C. S. *J. Magn. Reson., Ser. A* **1993**, *101*, 67−73.
(26) Heil, S. R.; Holz, M. *Angew. Chem., Int. Ed. Engl.* **1996**, *35*, 1717−1720.
(27) Fang, Y.; Yushmanov, P. V.; Furó, I. *Magn. Reson. Chem.* **2017**, *55*, 584−588.
(28) Mo, H.; Raftery, D. *J. Magn. Reson.* **2008**, *190*, 1−6.
(29) Bernstein, M. A.; Sýkora, S.; Peng, C.; Barba, A.; Cobas, C. *Anal. Chem.* **2013**, *85*, 5778−5786.
(30) Vadim Zorin, M. B. Felipe Seoane, Stanislav Sykora, Carlos Cobas. *SMASH*: Italy, 2017.
(31) Wu, D. H.; Chen, A. D.; Johnson, C. S. *J. Magn. Reson., Ser. A* **1995**, *115*, 260−264.
(32) Badertscher, M.; Bühlmann, P.; Pretsch, E. *Structure Determination of Organic Compounds, Tables of Spectral Data*, 4th ed.; Springer: Berlin, Heidelberg, 2009.
(33) Nishizaki, Y.; Lankin, D. C.; Chen, S.-N.; Pauli, G. F. *Anal. Chem.* **2021**, *93*, 2733−2741.
(34) Morris, G. A.; Barjat, H.; Home, T. J. *Prog. Nucl. Magn. Reson. Spectrosc.* **1997**, *31*, 197−257.
(35) Liu, M.; Tang, H.; Nicholson, J. K.; Lindon, J. C. *Magn. Reson. Chem.* **2002**, *40*, S83−S88.
(36) Lefebvre, B.; Corrin, T.; Simpson, A. J.; Shirzadi, A.; Burrow, T. E.; Dicks, A. P. *J. Chem. Educ.* **2009**, *86*, 360−362.
(37) Kan, L.-s.; Borer, P. N.; Cheng, D. M.; Ts'o, P. O. P. *Biopolymers* **1980**, *19*, 1641−1654.
(38) D'Amelio, N.; Fontanive, L.; Uggeri, F.; Suggi-Liverani, F.; Navarini, L. *Food Biophys.* **2009**, *4*, 321−330.
(39) Dauner, B. R.; Pringle, D. L. *J. Chem. Educ.* **2014**, *91*, 743−746.
(40) Zhou, Y.; Hu, K.; Shen, J.; Wu, X.; Cheng, G. *J. Mol. Struct.* **2009**, *921*, 150−155.
(41) Ohtsuki, T.; Sato, K.; Abe, Y.; Sugimoto, N.; Akiyama, H. *Talanta* **2015**, *131*, 712−718.
(42) Liu, M.; Nicholson, J. K.; Parkinson, J. A.; Lindon, J. C. *Anal. Chem.* **1997**, *69*, 1504−1509.
(43) Sokolenko, S.; Jézéquel, T.; Hajjar, G.; Farjon, J.; Akoka, S.; Giraudeau, P. *J. Magn. Reson.* **2019**, *298*, 91−100.
(44) Heikkinen, S.; Toikka, M. M.; Karhunen, P. T.; Kilpeläinen, I. A. *J. Am. Chem. Soc.* **2003**, *125*, 4362−4367.

https://doi.org/10.1021/acs.analchem.1c00831
Anal. Chem. 2021, 93, 9697−9703